Microstructure and Mechanical Properties of FeAl Intermetallics Prepared by Mechanical Alloying and Hot-Pressing[*]

SONG Haixia (宋海霞)[1,2], WU Yunxin (吴运新)[1,**], TANG Chuan'an (唐传安)[1],
YUAN Shuai (袁 帅)[1], GONG Qianming (巩前明)[1], LIANG Ji (梁 吉)[1]

1. Department of Mechanical Engineering, Tsinghua University, Beijing 100084, China;
2. Department of Mechanical Engineering, Army Aviation Institute of PLA, Beijing 101123, China

Abstract: FeAl intermetallics were prepared by mechanical alloying and vacuum hot-pressing. The Fe-48 at.% Al powder was ball-milled for 3-12 h, producing a solid solution structure of Fe (Al) with trace Al (Fe). Subsequent vacuum annealing or hot-pressing introduced phase transformations into the FeAl (B_2) intermetallics and Al_2O_3 inclusions. The hot-pressed FeAl intermetallics possess a high flexural strength of 831 MPa and a fairly good strain at break of 3.2%. The results show that the addition of 0.5 at.% B reduces the peak temperature for hot-pressing from 1180℃ to 1100℃, and increases the density of the compacts from 95% to 96.3%, but results in no significant improvement in the mechanical properties.

Key words: FeAl intermetallics; mechanical alloying; powder; hot-pressing; flexural strength

Introduction

FeAl intermetallics are becoming more and more attractive for materials engineering because of their excellent physical, chemical, and mechanical properties, i.e., low density, good corrosion and oxidation resistance, and high strength at both room and elevated temperatures[1-3]. It has been shown that with increasing Al concentration, the oxidation and sulphidization resistances of FeAl alloys increase, while their densities decrease[4]. This makes the FeAl intermetallics with high Al concentrations good candidates for structural materials for use in high-temperature, hostile environments. However, wide application of FeAl intermetallics has been limited by their inherently low ductility and toughness, especially at ambient temperatures. Higher percentages of Al in the FeAl intermetallics reduce the ductility[5,6] which makes fabrication by conventional techniques such as ingot metallurgy difficult[7].

Recent studies have demonstrated the feasibility of fabricating FeAl intermetallics by powder metallurgy (P/M), including hot isostatic pressing (HIP)[8], extruding[9,10], hot forging or pressing[11,12], and powder injection molding[13]. The FeAl powders used for P/M processes were prepared mostly by mechanical alloying (MA)[8-12]. The MA process avoids the complicated melting and solidification processes associated with powder atomization. In addition, the formation of nanocrystalline structures is possible in the ball-milled FeAl powders, thus helping improve the ductility[9]. Nevertheless, the microstructures and properties of mechanically alloyed FeAl are very dependent upon the ball-milling and P/M conditions[11,14-16]; therefore, more systematic research is necessary to correlate the processing conditions with the microstructure and properties.

In this work, the Fe-48 at.% Al powder was mechanically alloyed by high-energy ball milling and then consolidated by vacuum hot-pressing. The microstructural changes during ball milling and subsequent

consolidation were examined and the flexural behaviors were evaluated. The effect of elemental boron addition on the sintering and mechanical properties was also investigated.

1 Experimental

Electrolytic Fe and gas-atomized Al powders were used for the mechanical alloying. The powder particle sizes and chemical compositions are given in Table 1. The powders were mixed in a proportion of 52 at.% Fe: 48 at.% Al, with the mixture morphology shown in Fig. 1. Mechanical alloying was carried out using a planetary ball mill (QM-1SP2), with a ball-to-powder mass ratio of 10:1. Ethanol (0.5 wt.%) was added as a process control agent. To protect the powders against oxidation, argon was introduced into the vials. The powder mixture was milled at 304 r/min for 3-12 h, with an interval of 0.1 h per 0.4 h. After finishing, the vials were slowly cooled and opened in air, so that the powders were collected with exposure to air. The powders milled for different time periods were annealed at 1100℃ for 1 h in a vacuum furnace. X-ray diffraction (XRD) by a D/Max-RB diffractometer was performed before and after annealing to characterize the microstructural changes. The powder particle size was examined using a Laser Mastersizer 2000 and the morphology was examined using a JSM-6310F scanning electron microscope (SEM).

Table 1 Characteristics of the elemental Fe and Al powders

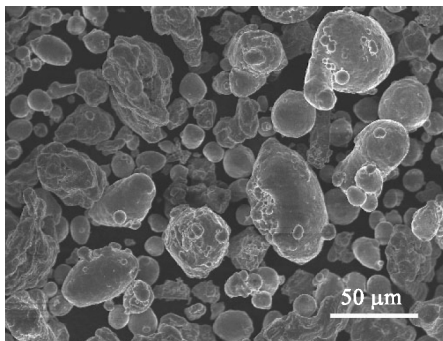| Powder	Particle size (μm)	Composition (wt.%)						
		Fe	Al	H_2O	C	O	Si	Mo
Fe	＜75	99.5	—	＜0.1	＜0.1	＜0.03	＜0.1	＜0.20
Al	＜45	—	99.9	＜0.1	—	—	—	＜0.05

Fig. 1   SEM morphology of Fe-48 at.% Al powder mixture

A ZT-30-20Y vacuum hot-press machine was used to consolidate the powder that had been milled for 12 h into graphite dies as samples 20 mm in diameter and 7 mm in height. The pressure was fixed at 32 MPa and the peak temperature was determined by reference to the displacement of the punches at a displacement speed of 0.0083 mm/s. The effect of boron addition on sintering and mechanical properties was evaluated by adding 0.5 at.% boron to the samples. All the samples were held at their peak temperatures for 1-1.5 h.

The densities of the hot-pressed samples were measured using Archimede's method, the microstructures were characterized by XRD and microscope observations, the hardness was tested on an MH-3 microhardness indenter and the three-point bending tests were done on an EHF-EG50KN.T-10L tester. The three-point bending specimens were rectangular bars 15 mm × 3 mm × 2 mm. Five specimens were tested for each composition, with their flexural strengths and strains at break averaged for the final results.

2 Results

2.1 Mechanical alloying and annealing of Fe-48 at.% Al powder

Figure 2 shows the XRD patterns for Fe-48 at.% Al powders milled for different time periods. Even after 12 h of ball milling, the intermetallic FeAl (B_2) structure that is common in FeAl alloys of high Al concentrations was not formed yet. Instead, the relative intensities of the diffraction peaks for Al (111) and Al (311) decreased significantly with increasing milling time, with the diffraction peaks for both Fe and Al broadened and shifted to lower diffraction angles. This means that the present milling conditions formed only a solid solution structure consisting of the dominant Fe (Al) and trace Al (Fe) even with 12 h of ball milling. Enayati and Salehi[15] studied the MA process of Fe-50 at.% Al in a planetary ball mill, reporting that FeAl intermetallic compounds did not form until 15 h milling, with a fully FeAl structure resulting after 30 h

milling. In the study of Morris-Muñoz et al.[11], FeAl was formed in Fe-50 at.% Al powder after only 8 h ball milling. These results indicate that the kinetics of the Fe-Al MA process is sensitive to the milling conditions and changes in these conditions can lead to significant differences in the phase transformation and final structure.
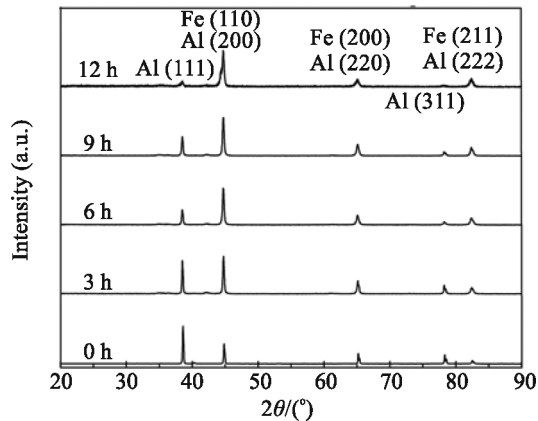

Fig. 2   XRD patterns for the Fe-48 at.% Al powders milled for different time periods

The variations of the powder particle size for various milling times are shown in Fig. 3. The particle size results are significantly refined in the first 6-h milling, indicating that the dominant milling mechanism is particle fracture in this stage. Prolonged milling beyond 6 h does not produce much more refinement in particle size, once a dynamic balance is achieved between particle fracture and cold welding. The nominal particle size, D_{50}, of the 12-h milled powder is 19.2 μm. D_{50} means that the cumulate volume percentage of ultra-fine particles whose granularity does not exceed D_{50} is 50% in all. D_{90} and D_{10} have similar means.
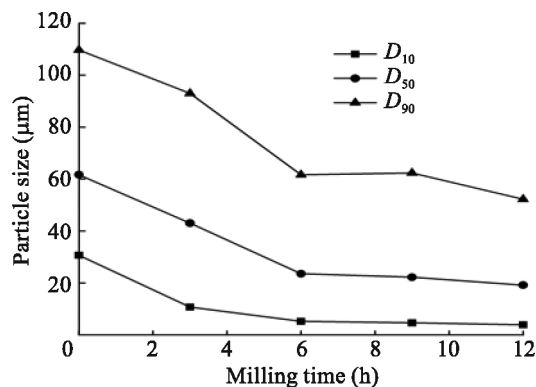

Fig. 3   Dependence of particle size on milling time for Fe-48 at.% Al powders

Figure 4 shows the SEM morphologies of Fe-48 at.% Al powders milled for 3 h and 12 h. Unlike the original round particles in the powder mixture shown in Fig. 1, the ball-milled powder becomes flaky and more irregular. In accordance with Fig. 3, the 12-h-milled powder is significantly finer than the 3-h-milled.
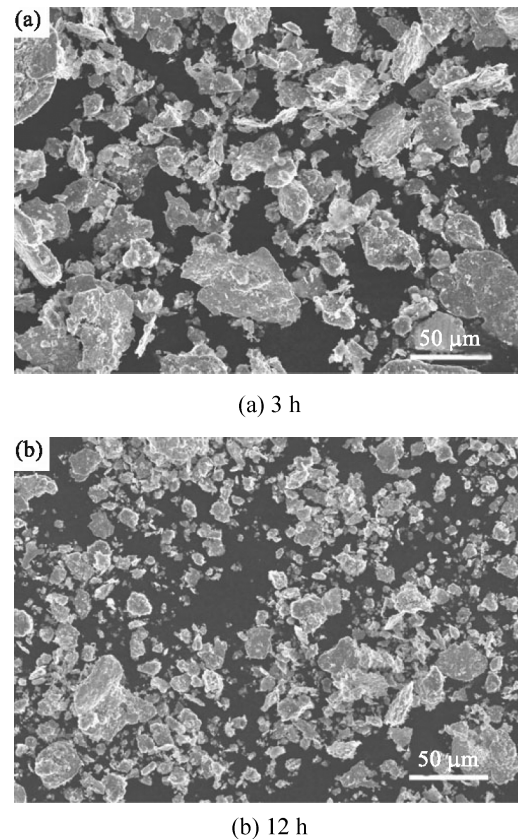

(a) 3 h

(b) 12 h

Fig. 4   SEM morphologies of Fe-48 at.% Al powders milled for (a) 3 h and (b) 12 h

Although the intermetallic FeAl (B2) structure is not formed in the as-milled powders, a phase transformation from Fe (Al) and Al (Fe) solid solutions to a FeAl (B2) intermetallic occurs during the subsequent vacuum annealing at 1100℃ for 1 h. As shown in Fig. 5, the structure of all the powders milled for 3 h to 12 h transformed to a dominant FeAl (B2) structure after the annealing heat treatment. This makes it possible to fabricate FeAl P/M parts directly from the as-milled powders, since the sintering of FeAl intermetallics usually occurs above 1100℃[13], which will be high enough to induce the intermetallic phase transformation. Furthermore, Fig. 5 also shows that a small amount of Al₂O₃ formed in the heat-treated powders. The formation of Al₂O₃ is associated with the oxygen

that is absorbed at the powder surface when exposed to air after ball milling. The detailed mechanism will be discussed later in this work.
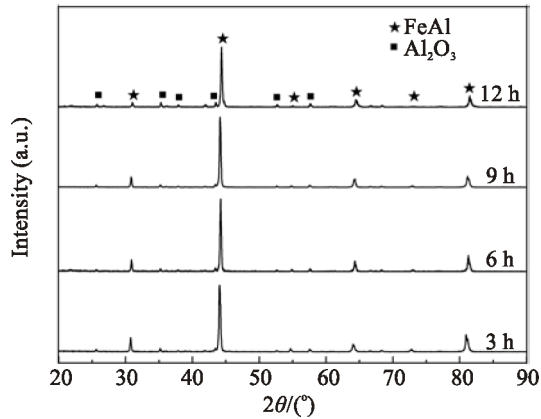

Fig. 5   XRD patterns for Fe-48 at.% Al powders milled for different time and then heat-treated

2.2   Microstructures of hot-pressed Fe-48 at.% Al intermetallics

The 12-h-milled powder was chosen for hot-pressing because of its finer particle size. The XRD patterns in Fig. 6 show a dominant FeAl (B_2) structure in the hot-pressed Fe-48 at.% Al, similar to those shown in Fig. 5. Although the addition of 0.5 at.% B does not make much difference to the sintered phase structure, the peak temperature for hot-pressing is greatly reduced from 1180℃ to 1100℃.
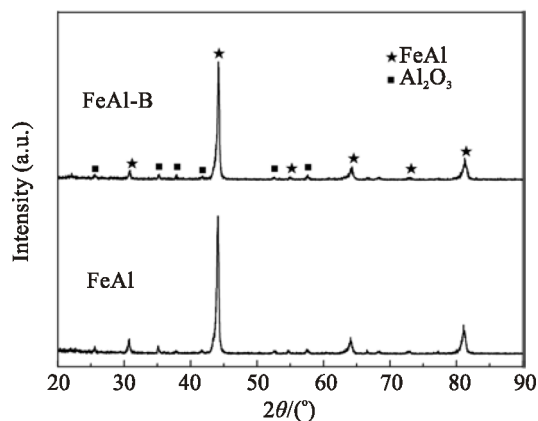

Fig. 6   XRD patterns for hot-pressed FeAl intermetallics

Figure 7 shows the micrographs of hot-pressed Fe-48 at.% Al and Fe-48 at.% Al-0.5 at.% B. Both compacts exhibit two microconstituents: elongated grains and fine particles surrounding the grains. The elongated grains are believed to be the intermetallic FeAl phase. The fine particles were verified as Al_2O_3

by the XRD measurement. Moreover, the SEM back-scattered image in Fig. 7d clearly shows an enrichment of light elements in the fine particles and subsequent energy dispersive X-ray (EDX) tests show that the major light element is oxygen.
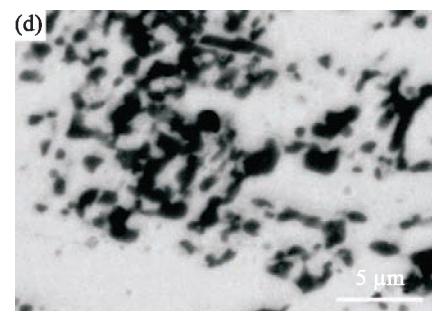

(a) Optical micrograph of FeAl
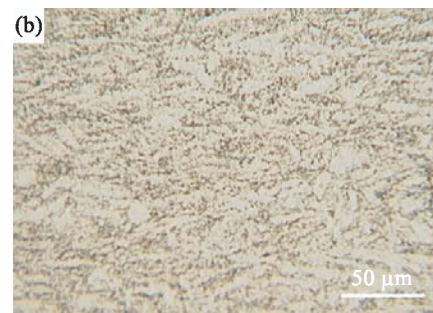
(b) Optical micrograph of FeAl-B
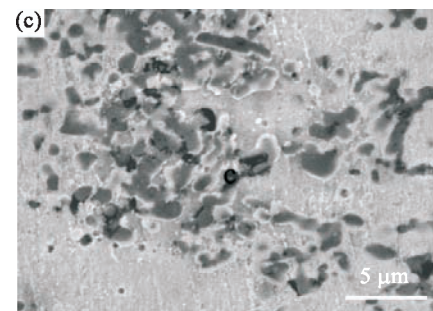
(c) SEM micrograph of FeAl

(d) Back-scattered image of Fig. 7c

Fig. 7   Microstructures of hot-pressed Fe-48 at.% Al intermetallics

In comparison, the FeAl grains in Fe-48 at.% Al-0.5 at.% B are finer and less directional, with fewer Al_2O_3 particles. This may be ascribed to the addition of boron, which reduces the sintering temperature, thus inhibiting FeAl grain growth and Al_2O_3 formation. Moreover, when the boron concentration percentage is beyond the solubility limit in Fe (about 10^{-4} (mass percentage)[17]), much boron is present in the form of Fe_2B, whose segregation in the grain boundaries also inhibits the FeAl grain growth[17,18].

2.3 Mechanical properties and fracture surfaces of hot-pressed Fe-48 at.% Al intermetallics

Table 2 lists the mechanical properties and relative densities of hot-pressed Fe-48 at.% Al and Fe-48 at.% Al-0.5 at.% B intermetallics. The densities of both materials are more than 95% of the theoretical (5.67 g/cm^3 for FeAl[12]), and the Fe-48 at.% Al-0.5 at.% B is a little denser, although it was hot-pressed at a lower peak temperature. The addition of 0.5 at.% boron did not significantly influence the flexural strength or the strain at break. Both materials exhibit a flexural strength of around 830 MPa and a strain at break of around 3.0%. However, the microhardnesses of the two materials are quite different. The Fe-48 at.% Al has a higher hardness, probably due to its higher Al_2O_3 concentration.

Table 2   Mechanical properties and relative densities of hot-pressed Fe-48 at.% Al intermetallics

Sample	Relative density (%)	Flexural strength (MPa)	Strain at break (%)	Microhardness (HV$_{100\,g}$)
FeAl	95.0	831.3	3.2	700
FeAl-B	96.3	828.9	3.1	600

The fracture surfaces of the two compacts are very irregular, as shown in Fig. 8. The fracture surface of FeAl consists of two different areas (Fig. 8a). The EDX analysis of typical regions in Fig. 9 and Table 3 clearly distinguishes the two areas. The large amount of finer grains exhibiting dimple-like fracture surfaces are FeAl grains, with Al_2O_3 particles distributed on these grains, while the large smooth areas with few pores correspond to the fracture surfaces of large FeAl grains. The pores may be produced by the pulling off of Al_2O_3 particles from the FeAl matrix. Debonding

can easily occur at the interface of the Al_2O_3 and FeAl matrix, so the in-situ formed Al_2O_3 particles contribute little to the strength[8]. The fracture surfaces of the B-containing material shown in Fig. 8b also include two areas similar to those of the Fe-48 at.% Al, but the FeAl grains are much finer and the smooth areas are smaller and less frequent, so the fracture surface appears more homogenous.
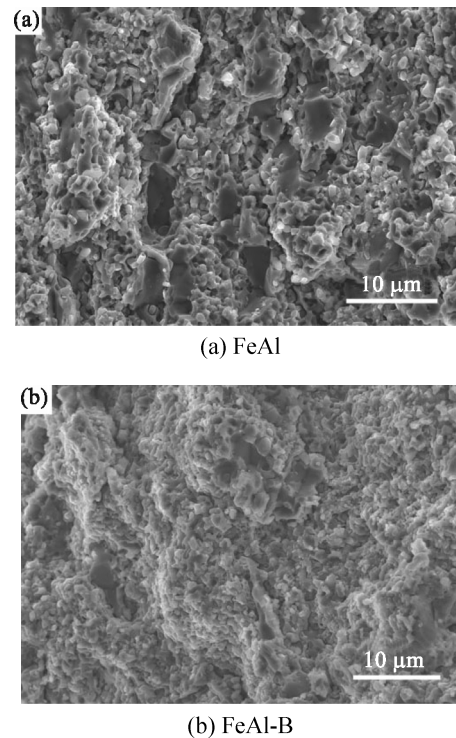

(a) FeAl

(b) FeAl-B

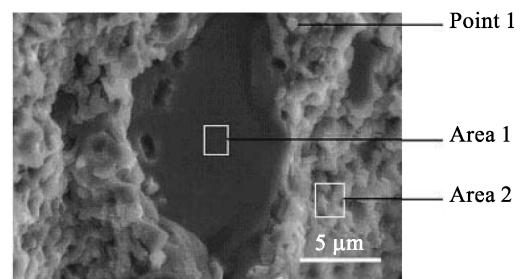**Fig. 8   Three-point-bending fracture surfaces of hot-pressed FeAl and FeAl-B**

Fig. 9   EDX of the fracture surface of hot-pressed FeAl

Table 3   EDX results corresponding to Fig. 9

Position	Element content (at.%)		
	Fe	Al	O
Point 1	13.80	4.49	58.99
Area 1	39.12	39.34	28.87
Area 2	45.50	6.18	10.77

3 Discussion

The formation of Al_2O_3 particles in both annealed and hot-pressed Fe-48 at.% Al is of particular interest. The oxygen may come from the elemental Fe and Al powders as well as contaminants on the vials, balls, and ethanol. However, these would contribute little to the total oxygen content in the final products. Most of the oxygen was probably from the surface oxygen absorption. As the milled powder was collected in air, oxygen was absorbed onto the fresh, high-energy powder surfaces. However, most Al_2O_3 is formed only at high temperatures, as shown by the XRD patterns for the milled powders before and after annealing or hot-pressing. A higher temperature promotes the formation of Al_2O_3, so the samples containing B have less Al_2O_3 than the Fe-48 at.% Al samples due to the lower peak temperatures for the hot-pressing.

The hot-pressed Fe-48 at.% Al exhibits a flexural strength of around 830 MPa and a strain at break of 3.2%. For comparison, the flexural strength of nanocrystalline FeAl prepared from mechanically alloyed powders followed by hot forging is no more than 650 MPa[11]. The strain at fracture break of FeAl alloy prepared by mechanical alloying of Fe-40 at.% Al powder followed by pneumatic isostatic forging was also 3.2%[19]. As reported by Deevi et al.[5,6], the ductility of FeAl alloys drops sharply with increasing Al concentration, especially when the Al content is over 45 at.%, and the Fe-48 at.% Al prepared by casting followed by hot-extruding also showed no observable plasticity. These results show that these Fe-48 at.% Al intermetallics prepared by mechanical alloying and hot-pressing possess relatively good mechanical properties.

The addition of B slightly increases the density of hot-pressed Fe-48 at.% Al, probably due to the smaller amount of Al_2O_3. The interface between the Al_2O_3 particles and FeAl matrix is relatively weak and the thermal expansion mismatch between FeAl and Al_2O_3 could cause debonding or cracking at the interface[20]. However, although the addition of 0.5 at.% B leads to finer grain size, there was no change to the flexural strength or the strain at break. According to Kim and Kwun[21], the addition of 1.2 at.% B did not improve the room-temperature tensile properties of mechanically alloyed and hot-extruded Fe-40 at.% Al alloy, but

actually reduced the strength. However, Muñoz-Morris et al.[17] found that B leads to considerable strengthening for concentrations not beyond the solubility limit in Fe (about 10^{-4} (mass percentage)) where boron exists in the form of a solid solution instead of the concentrated borides-Fe_2B. Though the amount of Fe_2B is too small to be detected by XRD and SEM, its segregation on the grain boundary leads to embrittlement of the boundary, which counteracts the effect of the finer grain size and the density, leading to no improvement in the flexural properties. The decrease in hardness of the B-containing materials is possibly attributed to its reduced Al_2O_3 content. The optimum B concentration will be examined in a future study.

4 Conclusions

The mechanically alloyed Fe-48 at.% Al powder has irregular, flaky shapes consisting of dominant Fe (Al) and trace Al (Fe) solid solutions. The phase transformations into the FeAl (B_2) intermetallic as well as into Al_2O_3 inclusions are induced by annealing or hot-pressing. The oxygen for the Al_2O_3 formation comes from surface absorption when the milled powder was exposed to air, with the reaction promoted by the high temperature processing.

The hot-pressed Fe-48 at.% Al materials exhibit good flexural properties, with a flexural strength of around 830 MPa and a strain at break of around 3.0%. The addition of 0.5 at.% B reduces the hot-pressing temperature and leads to a finer, more homogenous grain structure, but brings no improvement in the flexural properties.

References

[1] Grosdidier T, Ji G, Bernard F, Gaffet E, Munir Z A, Launois S. Synthesis of bulk FeAl nanostructured materials by HVOF spray forming and spark plasma sintering. *Intermetallics*, 2006, **14**(10&11): 1208-1213.

[2] Godlewska E, Szczepanik S, Mania R, Krawiarz J, Kozinski S. FeAl materials from intermetallic powders. *Intermetallics*, 2003, **11**(1&2): 307-312.

[3] Martinez M, Viguier B, Maugis P, Lacaze J. Relation between composition, microstructure and oxidation in iron aluminides. *Intermetallics*, 2006, **14**(10&11): 1214-1220.

[4] Varin R A, Bystrzycki J, Calka A. Characterization of nanocrystalline Fe-45 at.% Al intermetallic powders

obtained by controlled ball milling and the influence of annealing. *Intermetallics*, 1999, **7**(8): 917-930.

[5] Deevi S C, Sikka V K. Nickel and iron aluminides: An overview on properties, processing, and applications. *Intermetallics*, 1996, **4**(5): 357-375.

[6] Cohron J W, Lin Y, Zee R H, George E P. Room-temperature mechanical behavior of FeAl: Effects of stoichiometry, environment, and boron addition. *Acta Mater.*, 1998, **46**(17): 6245-6256.

[7] Koch C C, Whittenberger J D. Mechanical milling/alloying of intermetallics. *Intermetallics*, 1996, **4**(5): 339-355.

[8] Skoglund H, Wedel M K, Karlsson B. Processing of fine-grained mechanically alloyed FeAl. *Intermetallics*, 2004, **12**(7-9): 977-983.

[9] Morris D G, Gunther S. Strength and ductility of Fe-40Al alloy prepared by mechanical alloying. *Mater. Sci. Eng. A*, 1996, **208**(1): 7-19.

[10] Chao J, Morris D G, Muñoz-Morris M A, Gonzalez-Carrasco J L. The influence of some microstructural and test parameters on the tensile behaviour and the ductility of a mechanically-alloyed Fe-40Al alloy. *Intermetallics*, 2001, **9**(4): 299-308.

[11] Morris-Muñoz M A, Dodge A, Morris D G. Structure, strength and toughness of nanocrystalline FeAl. *NanoStruct. Mater.*, 1999, **11**(7): 873-885.

[12] Krasnowski M, Kulik T. Nanocrystalline FeAl intermetallic produced by mechanical alloying followed by hot-pressing consolidation. *Intermetallics*, 2007, **15**(2): 201-205.

[13] Kato K, Masui T. Influence of boron addition on the tensile properties of sintered FeAl compacts by powder injection molding. *Journal of the Japan Society of Powder and Powder Metallurgy*, 2002, **49**(9): 787-792.

[14] Bermudez M D, Carrion F J, Iglesias P, Martinez-Nicolas G, Herreraet E G, Rodriguez J A. Influence of milling condition on the wear resistance of mechanically alloyed aluminium. *Wear*, 2005, **258**(5&6): 906-914.

[15] Enayati M H, Salehi M. Formation mechanism of Fe_3Al and FeAl intermetallic compounds during mechanical alloying. *J. Mater. Sci.*, 2005, **40**(15): 3933-3938.

[16] Krasnowski M, Grabias A, Kulik T. Phase transformations during mechanical alloying of Fe-50%Al and subsequent heating of the milling product. *J. Alloys Compd.*, 2006, **424**(1&2): 119-127.

[17] Muñoz-Morris M A, Garcia Oca C, Morris D G. An analysis of strengthening mechanisms in a mechanically alloyed, oxide dispersion strengthened iron aluminide intermetallic. *Acta Mater.*, 2002, **50**(11): 2825-2836.

[18] Rico M M, Greneche J M, Perez-Alcazar G A. Effect of boron on structural and magnetic properties of the Fe60Al40 system prepared by mechanical alloying. *J. Alloys Compd.*, 2005, **398**(1&2): 26-32.

[19] Gedevanishvili S, Deevi S C. The effect of ZrO_2 grinding media on the attrition milling of FeAl with Y_2O_3. *Mater. Sci. Eng. A*, 2004, **369**(1&2): 236-240.

[20] Subramanian R, McKamey C G, Schneibel J H, Buck L R, Menchhofer P A. Iron aluminide-Al_2O_3 composites by in situ displacement reactions: Processing and mechanical properties. *Mater. Sci. Eng. A*, 1998, **254**(1-2): 119-128.

[21] Kim M H, Kwun S I. Tensile properties of cast and mechanically alloyed FeAl with high boron content. *Scripta Mater.*, 1996, **35**(3): 317-322.